AMERICAN SOCIETY FOR MICROBIOLOGY | Journal of Virology®

VACCINES AND ANTIVIRAL AGENTS

Rapid Elimination of Broadly Neutralizing Antibodies Correlates with Treatment Failure in the Acute Phase of Simian-Human Immunodeficiency Virus Infection

Yanling Wu,[a] Jing Xue,[b] Chunyu Wang,[a] Wei Li,[c] Lili Wang,[a] Weizao Chen,[c] Ponraj Prabakaran,[d] Desheng Kong,[e] Yujia Jin,[a] Dan Hu,[a] Yulu Wang,[a] Cheng Lei,[a] Diao Yu,[a,f] Chao Tu,[f] Ariola Bardhi,[g,h] Igor Sidorov,[i] Liying Ma,[e] Harris Goldstein,[g,h] Chuan Qin,[b] Lu Lu,[a] Shibo Jiang,[a] Dimiter S. Dimitrov,[c] Tianlei Ying[a]

[a]MOE/NHC/CAMS Key Laboratory of Medical Molecular Virology, School of Basic Medical Sciences, Shanghai Medical College, Fudan University, Shanghai, China

[b]Key Laboratory of Human Disease Comparative Medicine of Ministry of Health, Beijing Key Laboratory for Animal Models of Emerging and Re-emerging Infectious Diseases, Institute of Laboratory Animal Science, Chinese Academy of Medical Sciences (CAMS) and Comparative Medicine Center, Peking Union Medical College, Beijing, China

[c]Protein Interactions Section, Cancer and Inflammation Program, Center for Cancer Research, National Cancer Institute, National Institutes of Health, Frederick, Maryland, USA

[d]Intrexon Corporation, Germantown, Maryland, USA

[e]State Key Laboratory of Infectious Disease Prevention and Control, National Center for AIDS/STD Control and Prevention (NCAIDS), Chinese Center for Disease Control and Prevention, Beijing, China

[f]Biomissile Corporation, Shanghai, China

[g]Department of Microbiology and Immunology, Albert Einstein College of Medicine, Bronx, New York, USA

[h]Department of Pediatrics, Albert Einstein College of Medicine, Bronx, New York, USA

[i]Department of Medical Microbiology, Leiden University Medical Center, Leiden, The Netherlands

ABSTRACT Early human immunodeficiency virus type 1 (HIV-1) treatment during the acute period of infection can significantly limit the seeding of viral reservoirs and modify the course of disease. However, while a number of HIV-1 broadly neutralizing antibodies (bnAbs) have demonstrated remarkable efficacy as prophylaxis in macaques chronically infected with simian-human immunodeficiency virus (SHIV), intriguingly, their inhibitory effects were largely attenuated in the acute period of SHIV infection. To investigate the mechanism for the disparate performance of bnAbs in different periods of SHIV infection, we used LSEVh-LS-F, a bispecific bnAb targeting the CD4 binding site and CD4-induced epitopes, as a representative bnAb and assessed its potential therapeutic benefit in controlling virus replication in acutely or chronically SHIV-infected macaques. We found that a single infusion of LSEVh-LS-F resulted in rapid decline of plasma viral loads to undetectable levels without emergence of viral resistance in the chronically infected macaques. In contrast, the inhibitory effect was robust but transient in the acutely infected macaques, despite the fact that all macaques had comparable plasma viral loads initially. Infusing multiple doses of LSEVh-LS-F did not extend its inhibitory duration. Furthermore, the pharmacokinetics of the infused LSEVh-LS-F in the acutely SHIV-infected macaques significantly differed from that in the uninfected or chronically infected macaques. Host SHIV-specific immune responses may play a role in the viremia-dependent pharmacokinetics. Our results highlight the correlation between the fast clearance of infused bnAbs and the treatment failure in the acute period of SHIV infection and may have important implications for the therapeutic use of bnAbs to treat acute HIV infections.

IMPORTANCE Currently, there is no bnAb-based monotherapy that has been reported to clear the virus in the acute SHIV infection period. Since early HIV treatment is considered critical to restricting the establishment of viral reservoirs, investigation into the mechanism for treatment failure in acutely infected macaques would

Citation Wu Y, Xue J, Wang C, Li W, Wang L, Chen W, Prabakaran P, Kong D, Jin Y, Hu D, Wang Y, Lei C, Yu D, Tu C, Bardhi A, Sidorov I, Ma L, Goldstein H, Qin C, Lu L, Jiang S, Dimitrov DS, Ying T. 2019. Rapid elimination of broadly neutralizing antibodies correlates with treatment failure in the acute phase of simian-human immunodeficiency virus infection. J Virol 93:e01077-19. https://doi.org/10.1128/JVI.01077-19.

Editor Viviana Simon, Icahn School of Medicine at Mount Sinai

Address correspondence to Yanling Wu, yanlingwu@fudan.edu.cn, or Tianlei Ying, tlying@fudan.edu.cn.

Yanling Wu and Jing Xue contributed equally to this article.

Received 1 July 2019
Accepted 19 July 2019
Accepted manuscript posted online 2 August 2019
Published 30 September 2019

be important for the therapeutic use of bnAbs and eventually towards the functional cure of HIV/AIDS. Here we report the comparative study of the therapeutic efficacy of a bnAb in acutely and chronically SHIV-infected macaques. This study revealed the correlation between the fast clearance of infused bnAbs and treatment failure during the acute period of infection.

KEYWORDS HIV-1, acute SHIV infection, broadly neutralizing antibodies

Human immunodeficiency virus type 1 (HIV-1) continues to be a major public health problem, and new safer and more effective therapies are urgently needed. The early establishment of viral reservoirs is considered a major barrier in the development of approaches to cure HIV-1 infection (1, 2). Despite years of effective antiretroviral therapy (ART), these reservoirs persist and reinitiate infection after treatment is interrupted (3, 4). Therefore, treatment during the acute phase of HIV-1 infection provides a unique opportunity to prevent the establishment of these reservoirs and modify the course of disease.

Antibody-based therapeutics are typically more specific and relatively safer than most small-molecule drugs (5). In the past decade, a variety of potent broadly neutralizing antibodies (bnAbs) have been isolated from HIV-1-infected individuals, which has reinvigorated the concept of using antibodies to treat and eradicate HIV-1 infection (6). Of note, combinations of two or more bnAbs have been shown to provide improved neutralization breadth and potency, suppress the emergence of escape mutants during treatment, and induce durable suppression of plasma viremia (7–12). Recently, considering the extremely high cost of antibody cocktails, a new generation of bnAbs has also been designed by incorporating multiple antigenic specificities of neutralizing antibodies or engineered CD4 (eCD4) into a single antibody-like molecule (13–17). To date, these bnAbs have been extensively evaluated for their therapeutic potential *in vitro* and in animal models, especially in nonhuman primates infected with simian-human immunodeficiency virus (SHIV). However, although a number of bnAbs have demonstrated remarkable efficacy in preventing SHIV infection, or in reducing viremia in chronically SHIV-infected macaques, intriguingly, their inhibitory effects were substantially attenuated in the acute phase of SHIV infection. Only a few combinations of potent bnAbs or bnAb with ART showed therapeutic efficacy (18–20), and currently there is no bnAb-based monotherapy that has been reported to clear the virus in the acute SHIV infection period. Importantly, the mechanism for the disparate performance of bnAbs between the acute and chronic phases of SHIV infection remains elusive.

We previously engineered a bispecific multivalent bnAb consisting of the HIV-1 neutralizing antibody m36.4 coupled with the engineered single-domain eCD4 (21–23). This bispecific bnAb, designated LSEVh-LS-F (defucosylated LSEVh-LS), has been demonstrated to bind the CD4 binding site and CD4-induced epitopes on the HIV-1 envelope and neutralize all tested isolates, mediate potent antibody-dependent cellular cytotoxicity (ADCC) against HIV-1-infected cells, and effectively suppress HIV-1 infection in humanized mice (15, 23–25). In this study, using LSEVh-LS-F as a representative bnAb, we assessed its therapeutic effects in chronically SHIV-infected macaques as well as in macaques during the acute phase of SHIV infection. The pharmacokinetics (PK) of LSEVh-LS-F in uninfected macaques was also evaluated. Our data showed an unusually rapid decay of bnAbs in macaques with acute infection but not in chronically infected or uninfected macaques. This study suggested that the rapid exhaustion of antibodies may contribute to the treatment failure of bnAbs in macaques during the early acute phase of SHIV infection.

RESULTS

Long-term virological control by antibody therapy in chronically SHIV-infected rhesus macaques. To evaluate the therapeutic potential of LSEVh-LS-F, we infused a single dose of the antibody at 20 mg/kg of body weight into chronically SHIV-infected rhesus macaques. Four adult macaques were infected intravenously with $SHIV_{SF162P3}$

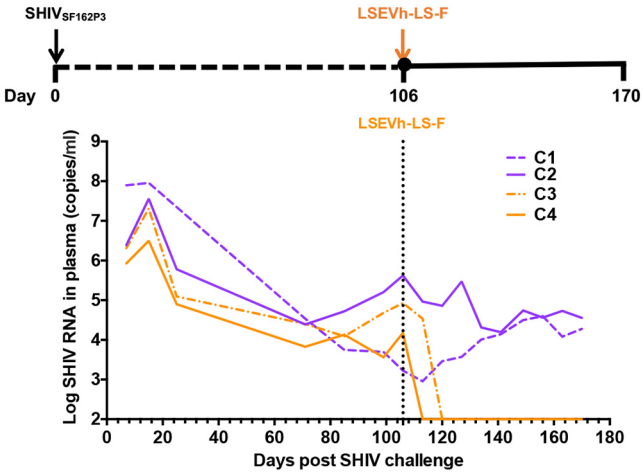

FIG 1 Suppression of plasma viremia after LSEVh-LS-F monotherapy in rhesus macaques chronically infected with $SHIV_{SF162P3}$. Four macaques were inoculated with 1,000 $TCID_{50}$ of $SHIV_{SF162P3}$ and treated with LSEVh-LS-F (orange) or PBS (purple) on day 106 after infection. Plasma viral RNA was measured by the RT-qPCR assay.

(1,000 50% tissue culture infective doses [$TCID_{50}$]) 106 days before the monoclonal antibody infusions. These animals exhibited chronic set point viral loads of 3.3 to 5.6 log RNA copies per ml. We performed a single infusion of LSEVh-LS-F on day 106 or used phosphate-buffered saline (PBS) as a contol, and plasma viral RNA levels were monitored for 10 weeks. We observed rapid and precipitous declines of plasma viral loads to undetectable levels after infusion of LSEVh-LS-F. In one monkey (C4) with baseline viral loads of about 4.2 log RNA copies per ml, plasma viremia was rapidly reduced to undetectable levels after antibody infusion. In another animal (C3) with higher baseline viral loads, about 4.9 log RNA copies per ml, the initial decline of plasma viremia was 0.4 log by day 7 and then viremia dropped rapidly to undetectable levels by day 14. In contrast, the plasma viremia of rhesus macaques in the control group was 4.1 to 4.5 log RNA copies per ml. Furthermore, the monkeys that received LSEVh-LS-F achieved complete virological suppression, and no viral rebound was observed for 10 weeks of the follow-up period (Fig. 1). Of note, virus rebound was often detected within one month after treatment with conventional HIV-1 bnAbs, such as 3BNC117 (26) and PGT121 (9). On the other hand, the combination of several different bnAbs, or engineered bi- or trispecific bnAbs, was able to reduce viral escape due to the enhanced neutralizing potency and breadth (27, 28). Similarly, as an engineered bnAb that has been shown to potently neutralize all tested HIV-1 and SHIV-1 isolates (15), LSEVh-LS-F used for therapy did not result in viral resistance in our study. These results demonstrate that a single-dose infusion of LSEVh-LS-F was able to provide sustained viral control in chronically SHIV-infected monkeys.

Significant but transient decrease of SHIV in acutely infected rhesus macaques by antibody therapy. Next, we sought to examine the therapeutic efficacy of LSEVh-LS-F during early acute $SHIV_{SF162P3}$ infection in rhesus macaques. To the best of our knowledge, to date there is no evidence that a bnAb would be able to eradicate acute SHIV infection if infused alone (not with other bnAbs or ART) to macaques. Consistently, we also found that a single dose of LSEVh-LS-F 7 days after SHIV inoculation has limited efficacy (24). To further explore the therapeutic performance of LSEVh-LS-F during the acute phase of SHIV infection, we administered multiple doses of antibodies and investigated whether such high-dose and continuous antibody treatment could suppress virus replication. Four macaques were inoculated intravenously with 1,000 $TCID_{50}$ of $SHIV_{SF162P3}$ and were administered intravenously four doses of LSEVh-LS-F ($n = 4$) on days 7, 9, 16, and 18 (Fig. 2A). Prior to treatment, the average plasma viremia levels were 3.9 and 4.2 log RNA copies per ml in the control and antibody groups, respec-

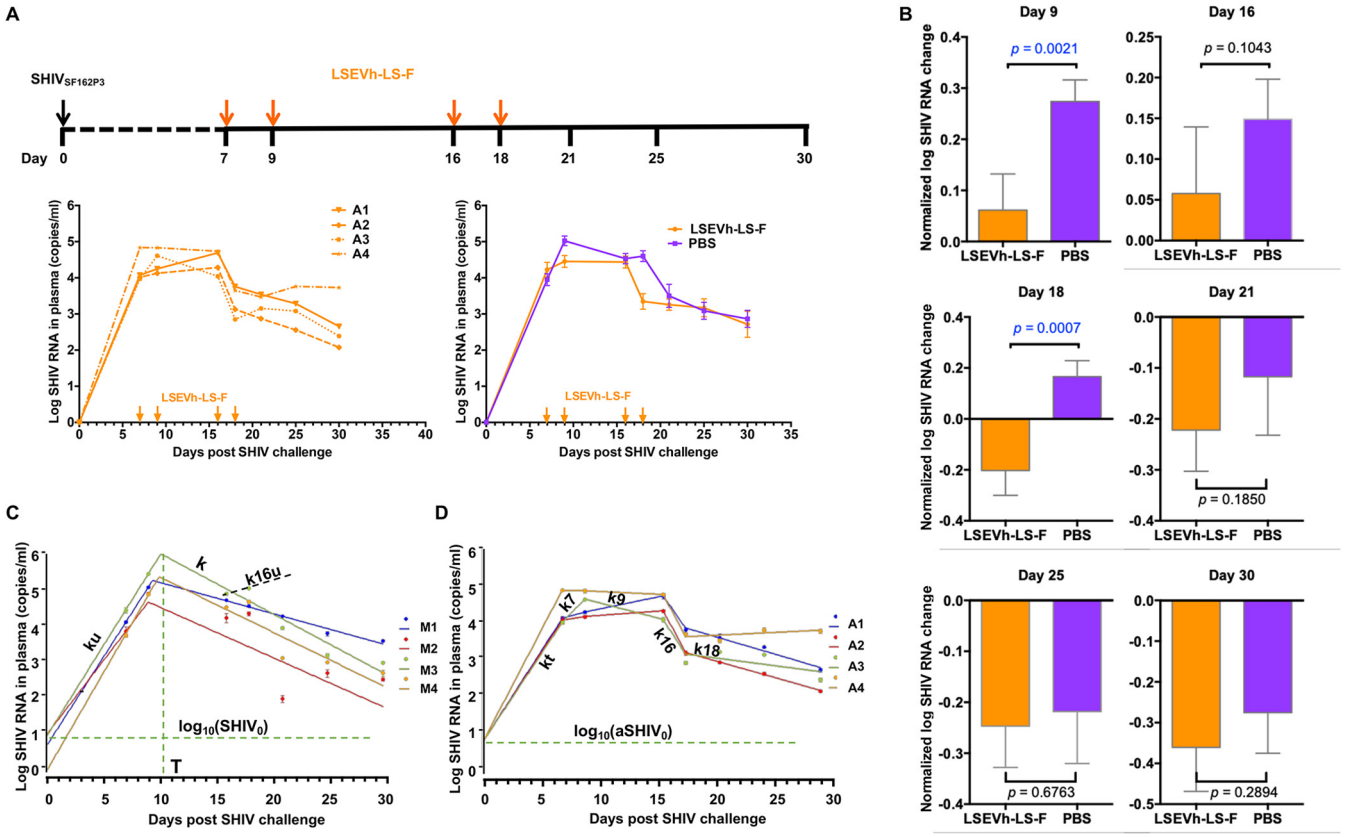

FIG 2 Therapeutic efficacy of LSEVh-LS-F in rhesus macaques during SHIV acute infection. (A) Experimental design of therapy experiment during the acute phase of SHIV infection. Eight rhesus macaques were challenged intravenously with SHIV$_{SF162P3}$ (1,000 TCID$_{50}$) and treated with 10 mg/kg of LSEVh-LS-F or PBS (n = 4 per group) on days 7, 9, 16, and 18. Plasma was collected at different time points (days 0, 7, 9, 16, 18, 21, 25, and 30). The orange arrows indicate the day of LESVh-LS-F administration. (B) Comparison of normalized plasma viral load (pVL) change at each time point, as determined by an unpaired two-tailed t test on log-transformed data. The error bars represent SDs for each group. (C) Data fitting for untreated macaques with mathematical models. Four constants were defined by data fitting: ku, k, T, and SHIV$_0$. Initial SHIV$_0$ load values and time of the viremia peak are shown by dashed lines. (D) Data fitting for treated macaques. Five constants were defined for each macaque by data fittings: kt, k7, k9, k16, and k18. SHIV$_0$ was fixed as the average value for untreated macaques.

tively, which were slightly lower than that in the above-mentioned chronically infected macaques (4.6 log RNA copies per ml). However, in contrast to the rapid elimination of viruses in the chronic phase of SHIV infection, even multiple administrations of LSEVh-LS-F in the acute phase resulted in only transient reduction in peak plasma viral loads, which was manifested by a 1-log$_{10}$ reduction, and decreased the viral replication to a short duration (2 days) compared to that of the PBS group (Fig. 2A).

To more precisely evaluate the efficacy of the treatment, we implemented a previously reported method to calculate the statistical significance of the difference between treated and untreated macaques (24). The virus RNA was normalized by dividing with the value of virus RNA on day 7 and subtracting 1. On day 9, 2 days after infusion of LSEVh-LS-F, we found a statistically significant decrease of viremia (P = 0.0021) (Fig. 2B). A significant decrease (P = 0.0007) of plasma viral load was also seen on day 18 when LSEVh-LS-F was also administered 2 days before the sample was taken (on day 16). However, this reduction of plasma viral load was transient, and 7 days after infusion of LSEVh-LS-F, a statistically significant decrease in plasma virus load was no longer evident.

To further confirm this analysis and provide additional quantitative information, we also explored an alternative mathematical model, which involves individually evaluating the infection kinetics for each animal and comparing virus RNA before drug administration and at different times thereafter. In this case, parameters used to fit the model to the experimental data for treated animals can be compared with those for untreated animals and conclusions can be drawn for the inhibitory effects. In addition,

TABLE 1 Rate constants for untreated macaques

Macaque	$SHIV_0$ (copies/ml)	ku (day^{-1})	T (days)	k (day^{-1})
M1	4.08 ± 0.96	1.13 ± 0.007	9.39 ± 0.22	−0.20 ± 0.005
M2	8.27 ± 0.16	0.94 ± 0.001	9.00 ± 0.00	−0.32 ± 0.000
M3	7.52 ± 1.23	1.16 ± 0.003	10.12 ± 0.09	−0.39 ± 0.001
M4	0.80 ± 0.01	1.25 ± 0.001	9.96 ± 0.06	−0.35 ± 0.001
Avg	5.17	1.12	9.62	−0.32

the results could allow fine-tuned analysis of infection kinetics, including comparison before and after the peak of viremia, with possible implications for understanding infection mechanisms. We have previously developed a mathematical model of HIV-1 infection kinetics in tissue cultures based on semiempirical functions which was successfully used to demonstrate the dominant role of HIV-1 cell-to-cell transmission and for evaluation of infection inhibitors (29). In this study, we use similar functions to fit the infection kinetics before and after the infection peak for infected and uninfected macaques by using three parameters: infection rate constant k, time to reach the infection peak T, and initial virus concentration (at time zero) (see Materials and Methods). These functions described very well the infection kinetics (Fig. 2C and D for untreated and treated macaques, respectively) and allowed us to determine two rate constants for untreated macaques, ku (rate constant before the peak) and k (after the peak) (Table 1), as well as four rate constants for treated macaques, including kt (before the peak), k7 (days 7 to 9), k9 (days 9 to 16), k16 (days 16 to 18), and k18 (days 18 to 30) (Table 2). In addition, we also analyzed the rate for untreated macaques from day 16 to day 18, as characterized by the rate constant k16u, which, for macaques 1, 2, 3, and 4, was found to be −0.18, 0.12, 0.18, and 0.17, respectively, on average, 0.074 day^{-1}.

We next used *t* test (unpaired, two-tailed, for two samples with unequal variance) to test the statistical differences between rates. In the interval from 0 to 7 days, no statistical difference was noted between kt and ku values for four treated and untreated monkeys ($P = 0.7040$; average values, 1.1573 and 1.1199, respectively) (Table 3). This result was expected because the rates of exponential increase of SHIV load in untreated and treated macaques before treatment should be similar. In the interval from 7 to 9 days, the dynamics of SHIV load in plasma for untreated macaques was still described by ku and for treated macaques by k7. A statistical difference can now be observed between ku and k7 values, $P = 0.0088$, and in this interval, k7 is smaller than ku (average values, 0.2578 and 1.1573, respectively) (Table 3). Importantly, this means that before the peak of viremia, treatment leads to statistically significant decrease in SHIV load rate of increase, even though SHIV still increases because the peak of viremia has not been reached. In the interval from 16 to 18 days, there was also significant statistical difference between k16u (untreated) and k16 (treated) ($P = 0.000041$) (Table 3).

Taken together, these results confirm that LSEVh-LS-F could provide evident but transient viral suppression during the acute phase of SHIV infection in rhesus macaques.

Pharmacokinetics of LSEVh-LS-F in uninfected rhesus macaques. We questioned whether the transient efficacy in acutely infected macaques resulted from the short

TABLE 2 Rate constants for treated macaques

Macaque	$aSHIV_0$ (copies/ml)[a]	kt (day^{-1})	k7 (day^{-1})	k9 (day^{-1})	k16 (day^{-1})	k18 (day^{-1})
A1	5.17	1.11 ± 0.006	0.20 ± 0.01	0.15 ± 0.005	−1.02 ± 0.02	−0.21 ± 0.01
A2	5.17	1.09 ± 0.019	0.12 ± 0.02	0.05 ± 0.021	−1.32 ± 0.06	−0.20 ± 0.02
A3	5.17	1.07 ± 0.005	0.73 ± 0.00	−0.19 ± 0.008	−1.10 ± 0.02	−0.10 ± 0.03
A4	5.17	1.36 ± 0.007	−0.02 ± 0.03	−0.03 ± 0.031	−1.34 ± 0.07	0.03 ± 0.05
Avg	5.17	1.16	0.26	−0.0048	−1.19	−0.12

[a]Fixed during the fitting.

TABLE 3 Statistical significance of difference between rate constants for treated and untreated macaques[a]

	Treated macaques					Untreated macaques		
Constant	kt	k7	k9	k16	k18	ku	k	k16u
kt		7.2E−03	2.2E−05	7.2E−07	9.4E−06	7.0E−01	1.0E−05	8.9E−05
k7			2.2E−01	9.6E−04	1.0E−01	8.8E−03	3.6E−02	3.7E−01
k9				3.6E−05	2.6E−01	2.4E−05	1.4E−02	5.1E−01
k16					7.1E−05	8.6E−07	3.7E−04	4.1E−05
k18						8.0E−06	3.4E−02	1.2E−01
ku							6.8E−06	1.1E−04
k								1.3E−02
k16u								

[a]Lack of significance ($P > 0.05$) is indicated by gray shading.

half-life of LSEVh-LS-F *in vivo*. To address this concern, we determined the pharmacokinetic parameters of LSEVh-LS-F in uninfected rhesus macaques. Three healthy macaques were intravenously administrated 10 mg/kg of LSEVh-LS-F, and serum samples were collected at 0, 2, 4, 8, 12, 24, 48, 72, 96, 120, 144, 168, 288, 408, 528, and 627 h postinfusion. The serum concentrations of LSEVh-LS-F at different time points were determined by enzyme-linked immunosorbent assay (ELISA). As shown in Fig. 3, LSEVh-LS-F displayed a pharmacokinetic profile typical of monoclonal antibodies, with a rapid distribution phase and a slower elimination phase. The *in vivo* antibody concentrations peaked up to 1,000 μg/ml 8 h following infusion, followed by prolonged elimination throughout the study period (26 days). Notably, the monkeys maintained LSEVh-LS-F levels in plasma exceeding its corresponding *in vitro* neutralization 50% inhibitory concentration (IC_{50}) (1.6 μg/ml) against $SHIV_{SF162P3}$ (the challenged SHIV strain in this study) even 10 days postinfusion. The pharmacokinetic parameters are shown in Table 4. LSEVh-LS-F displayed half-lives of 4.0, 3.0, and 3.8 days in three rhesus macaques, which are slightly shorter than but comparable to the half-lives of reported HIV-1 bnAbs in uninfected rhesus macaques (e.g., VRC01, 4.7 days, and N6-based trispecific antibody, 4.8 days) (28, 30, 31).

Infused LSEVh-LS-F levels in different SHIV-infected models. To further understand the disparate performance by antibody treatment, we compared the plasma concentrations of LSEVh-LS-F in chronic phases of SHIV infection with those in the acute infection phase. In chronically infected macaques, LSEVh-LS-F displayed a pharmacokinetics profile similar to that in uninfected macaques (Fig. 4A). Within 2 weeks of

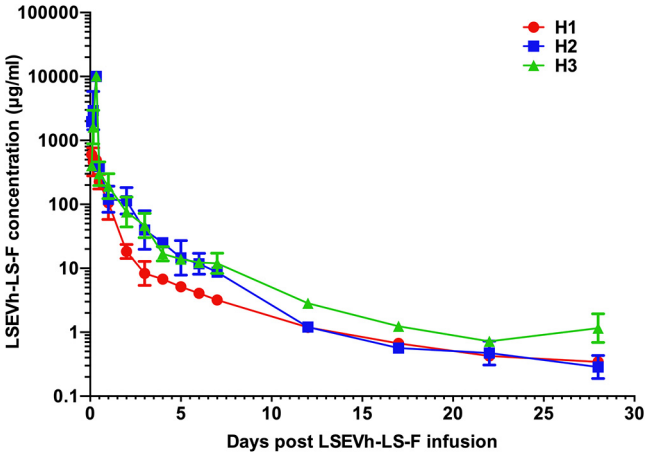

FIG 3 Pharmacokinetics of LSEVh-LS-F in uninfected macaques. A single intravenous administration of LSEVh-LS-F (10 mg/kg) was given to uninfected rhesus macaques ($n = 3$). Plasma levels of LSEVh-LS-F were measured by ELISA using $gp140_{sc}$ as the antigen and quantified by a standard curve drawn with known LSEVh-LS-F concentrations. The error bars indicate SDs.

TABLE 4 Pharmacokinetic parameters for LESVh-LS-F in uninfected macaques[a]

Macaque	C_{max} (μg/ml)	AUC_{0-t} (μg·h/ml)	CL (ml/h/kg)	$t_{1/2}$ (h)
H1	0.73×10^3	11×10^4	0.94	97
H2	10×10^3	69×10^4	0.15	72
H3	10×10^3	59×10^4	0.17	90

[a]The dose was 10 mg/kg for all macaques.

antibody infusion, the plasma concentrations of LSEVh-LS-F were maintained above its corresponding *in vitro* neutralization IC_{80} (3.9 μg/ml) against $SHIV_{SF162P3}$. The plasma viremia was rapidly controlled to undetectable levels without any rebound. The LSEVh-LS-F levels continued to decay slowly in the next 2 months to around 1 μg/ml at the end of study. However, viral suppression appeared less durable in the acutely SHIV-infected macaques, and surprisingly, we found that LSEVh-LS-F was much more rapidly cleared even with multiple antibody infusions (Fig. 4B). On day 9, 2 days after the administration of LSEVh-LS-F, its concentration was about 13 to 22 μg/ml, and a transient plasma viremia reduction was observed. At the next time point (day 16), 7 days after the second injection of LSEVh-LS-F, its concentration had dropped to below 1 μg/ml, which was insufficient to suppress viremia. Furthermore, with a third antibody infusion on day 16, the plasma LSEVh-LS-F concentration temporarily increased to above 4 μg/ml 2 days postinfusion but rapidly declined to undetectable levels ($<$0.1 μg/ml) even after the fourth antibody injection, and the viremia had rebounded to the same level as in control group. These results showed that the acutely SHIV-infected macaques significantly differed from uninfected and chronically infected macaques with respect to the pharmacokinetics of the infused LSEVh-LS-F.

Host humoral responses. To explore the mechanism underlying the viremia-dependent pharmacokinetics of LSEVh-LS-F, we compared the host humoral immune responses to infused LSEVh-LS-F in infected macaques with that in uninfected macaques. The macaque anti-human antibodies in serum samples were quantified by ELISA, and the samples before LESVh-LS-F infusion were used as negative controls. In all the macaques, we found that the anti-human antibodies began to appear in the first week and peaked approximately 10 days after the LESVh-LS-F infusion (Fig. 5A and B). No difference was evident between the healthy and infected macaques with respect to the development pattern and level of anti-LESVh-LS-F antibodies. Therefore, the fast elimination of LSEVh-LS-F in acutely SHIV-infected rhesus macaques was not due to the development of anti-drug antibodies.

It has been reported that endogenous antibodies may play an important role in the efficacy of passive immunotherapies (32, 33). Therefore, we also investigated the development of SHIV-specific antibodies in the infected macaques. The anti-SHIV antibodies in serum were measured by ELISA using $gp140_{sc}$ as the antigen and peroxidase-labeled anti-macaque IgG as the secondary antibody. Interestingly, very few SHIV-specific antibodies could be detected in the acute infection period. A large number of $gp140_{sc}$-specific macaque antibodies were generated 3 to 4 weeks after SHIV challenge, and their levels plateaued after 5 to 6 weeks (Fig. 5C).

Notably, antigen-dependent pharmacokinetics has also been observed in anti-tumor antibodies (34) and another anti-HIV-1 bnAb, 3BNC117 (35). It has been speculated that the faster decay of antibodies in the presence of antigens is due to the accelerated clearance of antigen-antibody complexes. Such a mechanism could also explain the fast exhaustion of infused bnAbs in the acute phase of SHIV infection observed in this study. Although further investigation is required, based on our findings we speculate that the endogenous SHIV-specific antibodies, maintained at high levels in the chronically SHIV-infected macaques, may play a modulating role and compromise the elimination of infused bnAbs by SHIV (Fig. 6).

DISCUSSION

Attempts to use anti-HIV-1 bnAbs alone, in combination, or as components of chimeric antigen receptors (CARs), bispecific T cell engagers (BiTEs), and other bispecific

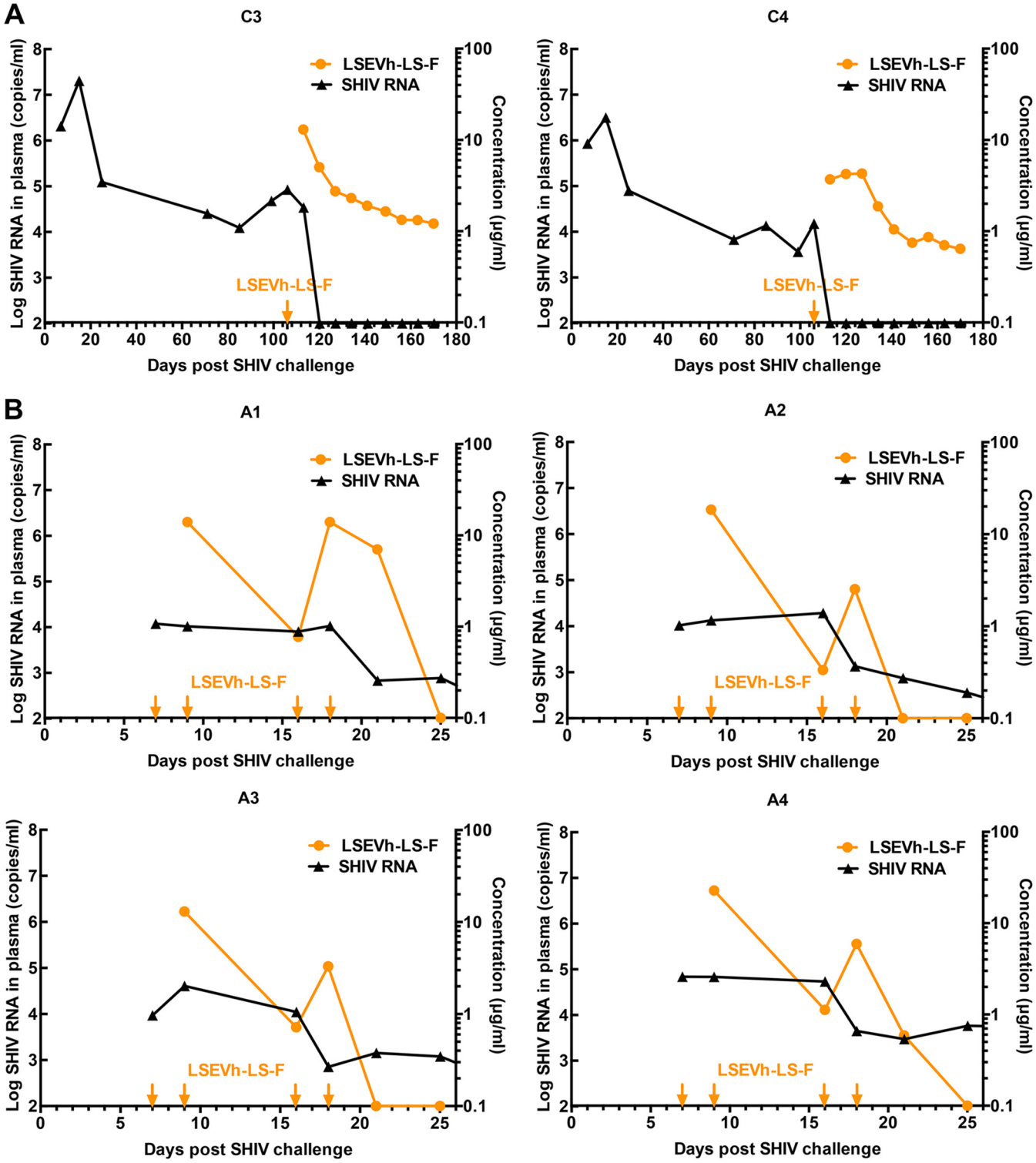

FIG 4 Plasma viral loads (black) and LSEVh-LS-F concentrations (orange) in two chronically (A) or four acutely (B) SHIV-infected rhesus macaques.

proteins have shown promising *in vitro* and *in vivo* results (36–39). However, resistance has been reported for various bnAbs targeting multiple sites, including V1/V2, V3, and the CD4 binding site. Bouvin-Pley et al. reported that HIV-1 clade B has increased resistance towards bnAbs targeting gp120, as shown by VRC01, NIH45-46, PG9, PG16, PGT121, and PGT128 (40). Previous studies with humanized mice, macaques, and

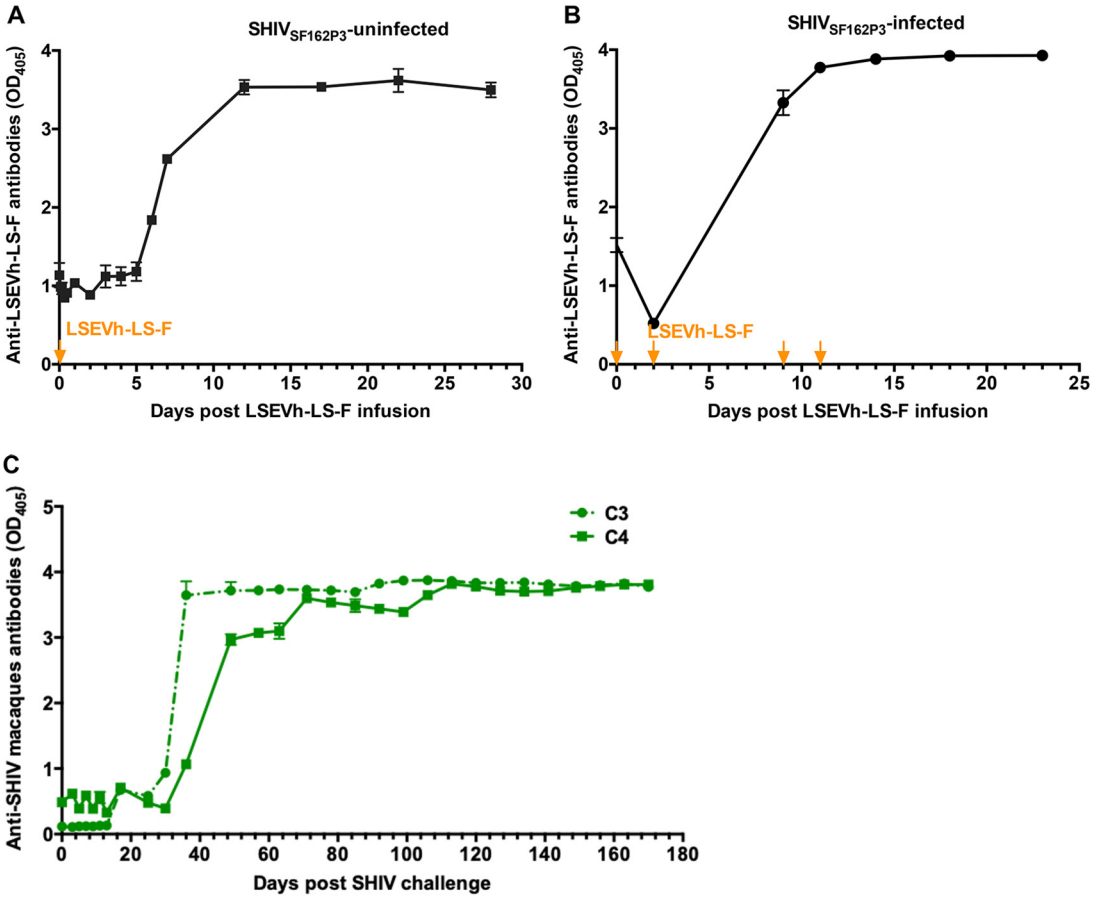

FIG 5 Host humoral responses to bnAb and SHIV challenge. The plasma reactivities to LSEVh-LS-F in uninfected (A) and SHIV-infected (B) animals were determined by using an ELISA-based approach. Arrows indicate the timing of LSEVh-LS-F infusion. (C) Endogenous antibodies against SHIV gp140 in macaques C3 and C4. The anti-SHIV antibodies in serum were measured by ELISA, and peroxidase-labeled anti-macaque IgG was used as the detecting antibody.

humans showed that a number of single monoclonal antibodies were unable to control viremia and resulted in rapid reemergence of resistance. Shingai et al. reported that antibody 10-1074, a bnAb targeting the CD4 binding site, caused a rapid decline in virus load to undetectable levels for 4 to 7 days when administered individually to infected macaques, followed by virus rebound on day 10 (26). The single glycan-dependent monoclonal antibody PGT121 resulted in complete suppression of chronic SHIV viremia, followed by viral rebound in most animals after a median of 56 days (9). These findings have led to the engineering of a new generation of bispecific or multispecific bnAbs. For instance, Xu et al. reported that a trispecific bnAb conferred complete immunity against a mixture of SHIVs in macaques that otherwise show resistance to single monospecific bnAbs (28). Recent studies also demonstrated the robust and sustained antiviral effects of engineered bnAbs with eCD4 as a component, given the fact that all HIV-1 isolates, including those few which can enter cells using only a coreceptor, bind to the primary HIV-1 receptor CD4 (41). In this study, we observed that a single-dose infusion of the bispecific multivalent eCD4-based bnAb LSEVh-LS-F resulted in rapid virological control in chronically SHIV-infected macaques without the development of resistance. Such profound virological suppression may reflect the importance of pursuing bispecific or multispecific targeting in bnAb-mediated treatment of HIV-1.

HIV-1-infected patients require combination ART (cART) treatment for life mainly because the virus persists in the latent viral reservoir. A recent study reported that cART initiated as early as 5 days after HIV-1 challenge failed to prevent viral rebound in

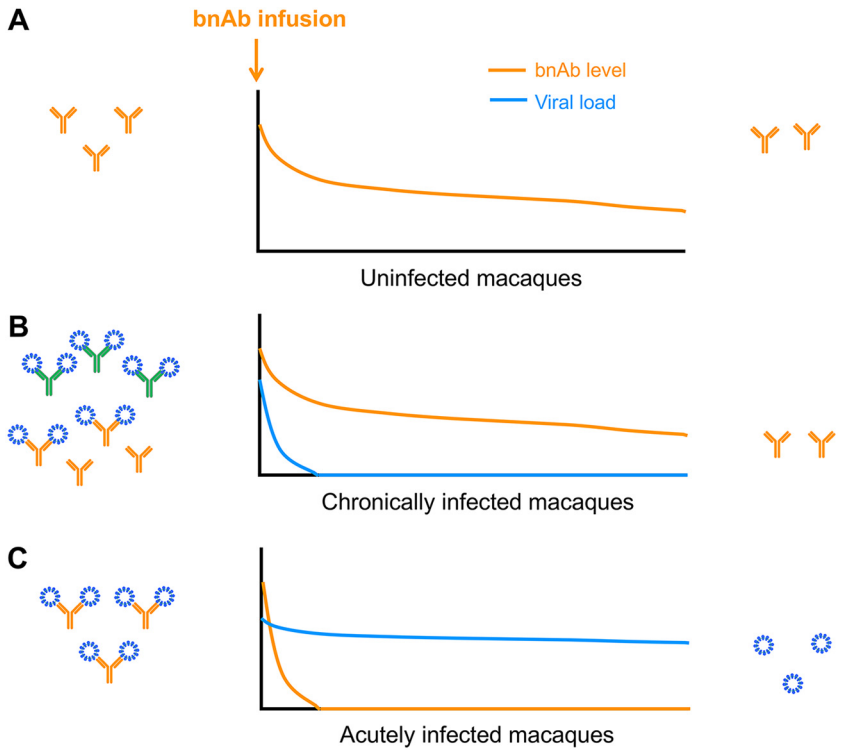

FIG 6 Representative mechanism for the decay of infused bnAbs in different SHIV infection groups: uninfected (A) and chronically (B) and acutely (C) infected macaques. The SHIV particles are shown in blue. The infused bnAbs are shown in orange, and endogenous SHIV-specific antibodies are shown in green.

humanized mice, indicating that viral latency had been established prior to peak viremia (10). Therefore, therapeutic intervention is likely more promising during the acute infection period. In this regard, the use of bnAbs is advantageous not only because of their superior neutralizing potency and breadth but also because they have the potential to restrict or eliminate the viral reservoirs by inducing antibody-mediated effector functions and immune responses against infected cells, including ADCC, antibody-dependent cellular phagocytosis (ADCP), and complement-dependent cytotoxicity (CDC). However, despite their substantial therapeutic efficacy in chronically SHIV-infected macaques, most of the reported bnAbs failed to show consistent benefit when administrated during the acute phase of SHIV infection. A current priority is to understand what has caused such disparate outcomes in different SHIV infection periods and translate this information into the development of more effective antibody therapeutics against HIV-1.

For the first time, Bolton and colleagues recently demonstrated that infusion of a combination of two potent bnAbs during early acute $SHIV_{SF162P3}$ infection in rhesus macaques potently suppresses acute SHIV plasma viremia and reduces CD4 T cell-associated viral DNA (18). In that study, SHIV-sensitive bNAbs were administered at a relatively high dose (40 mg/kg) on day 10 after challenge with 20 $TCID_{50}$ of SHIV, and then received daily cART treatment beginning on day 21. The combination of VRC07-523 and PGT121 infusions resulted in 1- to 1.5-log reduction in peak plasma viral loads during the initial 11-day treatment window. In contrast to the study by Bolton et al., in our study macaques were challenged with 1,000 $TCID_{50}$ of SHIV, i.e., 50-fold more than 20 $TCID_{50}$, and subsequently administered multiple doses of LSEVh-LS-F, each one at one-fourth the bnAb dose used (10 mg/kg versus 40 mg/kg). Our data showed robust (1-log) *in vivo* activity during acute $SHIV_{SF162P3}$ infection, but antiviral activity was sustained for just 2 days. In another recent study, greater acute viremia control was observed with a combination of two other potent bnAbs (3BNC117 and 10-1074) when

administered on days 3, 10, and 17 after $SHIV_{AD8\text{-}EO}$ infection, and long-term suppression (56 to 177 days) of viremia was achieved (19). The IC_{50}s of 10-1074 and 3BNC117 against SHIV were 0.2 μg/ml and 0.14 μg/ml, respectively (26). LSEVh-LS-F possesses less potent neutralization of SHIV, with an IC_{50} of 1.6 μg/ml (24). In addition, in uninfected macaques, 3BNC117 and 10-1074 showed median half-lives of 1.45 and 1.05 weeks, respectively (42), whereas LSEVh-LS-F showed a shorter half-life, 0.51 week, in uninfected macaques. Importantly, baseline viral load levels before antibody administration may also affect therapeutic potential. Taken together, these studies indicate that therapeutic efficacy *in vivo* was associated with neutralizing activity and half-life. The reduced inhibition of acute viral replication by bnAbs, to some extent, suggests that the therapeutic approaches during the acute viral infection period should be further investigated. For example, combination with cART and treatment as early as possible could achieve acute viremia control.

One major finding of this study was the significantly faster decay of bnAb LSEVh-LS-F in the acutely SHIV-infected macaques versus in the chronically infected or uninfected macaques. Interestingly, faster decay of bnAbs in HIV-1-infected patients was also described previously, and the accelerated clearance of antigen-antibody complexes was speculated to have caused the fast antibody elimination in the presence of HIV-1 (27, 28). Notably, in our study the chronically infected macaques had plasma viremia levels (4.6 log RNA copies per ml) prior to antibody treatment comparable to those in acutely infected macaques (4.2 log RNA copies per ml). These animals retained a relatively high-level serum concentration of LSEVh-LS-F and maintained long-term virological control (Fig. 4). We assume that the elimination of LSEVh-LS-F not only was attributable to the presence of substantial viral antigens but also relied on the host antiviral immune responses. The endogenous SHIV-specific antibodies were not developed until 3 to 4 weeks post-viral challenge and were maintained at high levels thereafter. It is possible that these endogenous antibodies played a role in depleting SHIV antigens and compromised the elimination effects of the viruses on the infused bnAbs. Defining the precise immunological mechanisms for these observations would be important to understand the viremia-dependent pharmacokinetics of bnAbs in macaques and thus warrants further investigation.

In our study, the bnAb LSEVh-LS-F displayed rapid antibody clearance in the acutely infected macaques and its inhibitory effect had a short duration, but it still exhibited potent activity for several days after administration. We have previously found that an exponential decrease with rate constant 0.21 day^{-1} calculated for HIV-1 dynamics during 6 days after cART treatment for humans separates poor and good responders, i.e., more than 95% of patients with a rate constant of >0.28 day^{-1} were good responders (43). This value can be compared with k16 values in the current experiments with macaques for the interval from 16 to 18 days, which corresponds to the after-peak treatment. Importantly, the absolute value of the rate constant k16 (average $= -1.2$ day^{-1}, varying in the range from -1.0 to -1.3 day^{-1}), 1.2, is larger than 0.21. For the untreated macaques the average k16u is 0.074 day^{-1}, which is close to zero. Based on the above-described analysis, it appears that the treatment in this case was more effective in decreasing SHIV load than cART treatment during the first 2 days of treatment. It is also higher than the rate constants we calculated for the chronically SHIV-infected macaques treated with the bnAbs 3BNC117 and 10-1074, which ranged from 0.36 to 0.89 day^{-1} (44). These results indicate that the treatment was effective in the acutely SHIV-infected macaques, and the short duration of suppression was largely due to the fast decay of the bnAb. Therefore, future engineering endeavors should aim to improve not only the neutralizing potency but also the half-life of the passive antibody, which could lead to the development of bnAb-based monotherapy capable of eliminating the virus in the acute SHIV infection period.

Interestingly, the effective rate constant k16eff (k16 – k16u) after the infection peak (1.27 day^{-1}) is also higher than the absolute value of the effective rate constant k7eff (k7 – ku) $= 0.26 - 1.1 = -0.84$ day^{-1} before the peak. This indicates that this inhibitor appears to be more effective during the quasi-steady state after the infection peak than

before the peak. Whether this difference is reproducible and valid for other inhibitors remains to be seen. The mechanism of such difference, if real, remains unknown. It can be speculated that it is related to differences in the infection kinetics, susceptibility to infection, and immune responses before and after the peak.

In conclusion, our data demonstrate that the transient, albeit significant, viral suppression by the bnAb LSEVh-LS-F was due to rapid antibody elimination during acute SHIV infection. The macaque SHIV-specific humoral immunity may play a role in the viremia-dependent pharmacokinetics of the bnAb, and the detailed mechanisms remain to be determined. Nonetheless, the findings of this study imply that it is critical to improve the duration of action of bnAbs in order to achieve successful treatment of acute SHIV/HIV-1 infection.

MATERIALS AND METHODS

Antibodies, viruses, and cells. Horseradish peroxidase (HRP)-conjugated anti-human Fc antibody was purchased from Sigma-Aldrich (St. Louis, MO). Horseradish peroxidase-conjugated mouse anti-IgG macaque pan-species was purchased from Kerafast (Boston, MA). Mouse CD4 monoclonal antibody was purchased from Abcam. The following cell lines were purchased: HEK293T cells were obtained from the ATCC, and 293 freestyle and CHO cells were obtained from Invitrogen-Life Technologies (Grand Island, NY). $gp140_{sc}$ protein was produced in our laboratory. Viral stocks of SHIV isolate SF162P3 were provided by the Beijing Institute of Animal Studies. The viruses were transferred into HEK293T cells, and culture supernatants were harvested after 48 h. The 50% tissue culture infective doses ($TCID_{50}$) were determined by TZM-bl assay.

LSEVh-LS-F preparation. Defucosylated LSEVh-LS (LSEVh-LS-F) was produced as described previously (24). Briefly, it was expressed in CHO-F6 cells which had their GDP-fucose transporter (GFT) genes inactivated using the genome editing system (45). It was purified by protein A Sepharose 4 FF column chromatography (GE Healthcare) as described previously (46). CHO-F6 cells were adapted for growth in serum-free Opti-CHO medium and were transfected with the LSEVh-LS vector. Stable cell lines producing LSEVh-LS-F were acquired by the standard glutamine synthetase-based selection system (47).

Antibody LSEVh-LS-F pharmacokinetics in SHIV-infected or uninfected rhesus macaques. In a single-dose PK study, three uninfected macaques were intravenously administered with LSEVh-LS-F at 10 mg/kg, and then serum samples were collected at 16 time points (0, 2, 4, 8, 12, 24, 48, 72, 96, 120, 144, 168, 288, 408, 528, and 627 h) after infusion. All experimental protocols were reviewed and approved by the institutional committee of Fudan University in accordance with the animal ethics guidelines of the Chinese National Health and Medical Research Council (NHMRC). Two adult rhesus monkeys were infected intravenously with $SHIV_{SF162P3}$ (1,000 $TCID_{50}$) for 106 days and received a single infusion of 20 mg/kg of LSEVh-LS-F, and plasma samples were collected at 10 time points before and after infusion. Four macaques were administered intravenously with 10 mg/kg of LSEVh-LS-F on day 7 post-SHIV challenges, and plasma samples were collected on days 0, 7, 9, 16, 18, 21, 25, and 30. Quantitative ELISA was used to determine the concentration of LSEVh-LS-F in the macaque plasma obtained at the different time points.

For measurement of serum antibody levels from uninfected macaques, 100 ng of $gp140_{sc}$ protein was used to coat half of 96-well ELISA (Costar; number 3690) plates overnight at 4°C. For serum samples from SHIV-infected macaques, these animals generated antibodies against HIV-1; thus, $gp140_{sc}$ proteins were not used as antigens. Because LSEVh-LS-F is composed of the CD4 domain, mouse CD4 monoclonal antibody was used to coat ELISA plates and incubated at 4°C overnight. These plates were washed with PBST buffer (PBS containing 0.5% Tween 20) and blocked with 3% (mass/vol) milk-PBS for 1 h at 37°C. After blocking, the serum samples and serial dilutions of purified LSEVh-LS-F were added and incubated for 1.5 h at 37°C. The standard curve was measured by a 3-fold dilution of antibody LSEVh-LS-F (initial 1 mg/ml) in PBS solution containing 5% macaque serum. Bound LSEVh-LS-F in serum was detected with horseradish peroxidase-conjugated anti-human Fc antibody, followed by the addition of 2,2′-azinobis(3-ethylbenzthiazolinesulfonic acid) (ABTS) substrate. The absorbance was read at 405 nm. The optical densities (OD) of a set of LSEVh-LS-F concentration standards were determined and used to plot an OD-versus-concentration standard curve that was analyzed by a four-parameter curve fit. The serum concentrations of LSEVh-LS-F were calculated from the standard curve, and the serum half-lives were analyzed on the basis of the concentrations of the LSEVh-LS-F measured at different time points after infusion using a noncompartmental pharmacokinetics data analysis model by Pharmacokinetics and Metabolism software (Summit Research Services).

SHIV infection and treatment design. Healthy male and female Chinese-origin rhesus macaques were randomly assigned to the study groups and challenged intravenously with $SHIV_{SF162P3}$ (1,000 $TCID_{50}$). For chronic infections, four adult rhesus monkeys were infected for 106 days, and two of them received a single infusion of LSEVh-LS-F at 20 mg/kg. For acutely infections, four doses of LSEVh-LS-F (10 mg/kg) were intravenously administered to macaques on days 7, 9, 16, and 18 after SHIV challenge. The monkeys in control groups were given PBS. Serum was collected at different time points for measurement of LSEVh-LS-F levels and other parameters. The research was conducted in an accredited Association for Assessment and Accreditation of Laboratory Animal Care (AAALAC) facility at the Institute of Laboratory Animal Science, Chinese Academy of Medical Sciences (Animal Experimental Approval

number XJ16002). All animals were anesthetized with ketamine hydrochloride (10 mg/kg) prior to the procedures. The experiments were performed in a biosafety level 3 laboratory.

Plasma viral load. SHIV RNA from plasma was purified using the QIAamp viral RNA minikit (Qiagen). The viral RNA loads in plasma were measured by quantitative reverse transcription-PCR (RT-qPCR) using a QuantiNova probe PCR kit (Qiagen) in an Eppendorf instrument. In the reverse transcription step, the nested reverse primer (SIVnestR01 [GTTGGTCTACTTGTTTTTGGCATAGTTTC]), instead of random hexamers, was used to facilitate priming of specific target sequences. Five microliters of the RT reaction mixture was added to a 20-μl reaction volume, and the quantitative PCRs were performed using a cycling protocol consisting of 95°C for 10 s and 60°C for 1 min. Primers and probe used for quantitative PCR were SGAG21 forward (5′-GTCTGCGTCATPTGGTGCATTC-3′), SGAG22 reverse (5′-CACTAGKTGTCTCTGCACTATPTGTTTTG-3′), and pSGAG23 (5′-6-carboxyfluorescein [FAM]-CTTCPTCAGTKTGTTTCACTTTCTCTTCTGCG-black hole quencher 1 [BHQ1]-3′) (20).

Humoral responses. Detection of polyclonal antibodies to LSEVh-LS-F in serum after infusion or anti-HIV-1 gp140 antibodies after SHIV challenge in chronically SHIV-infected macaques was performed using ELISA. LSEVh-LS-F or $gp140_{sc}$ was used for coating overnight, and diluted serum was incubated for 1.5 h, along with HRP-conjugated mouse anti-IgG macaque pan-species (Kerafast), with minimal cross-reactivity to human to avoid detection of LSEVh-LS-F.

Statistical analyses. Determination of statistical differences for viral load measurements was performed by unpaired two-tailed *t* test.

Mathematical model. A mathematical model similar to one based on exponential functions, as previously described (29), was used, and it is described below. For untreated macaques, we used two intervals: before the peak of viremia, interval 0 to T days (value of T is the model parameter defined by data fitting) and after the peak of viremia, interval T to 30 days. For treated macaques, the model describes SHIV dynamics during the interval when no treatment was done, or 0 to 7 days, and in four other intervals when Ab treatments were done, or 7 to 9, 9 to 16, 16 to 18, and 18 to 30 days. In each shown interval for both treated and untreated macaques, SHIV dynamics are described by a simple exponential model in which the initial value is defined by the SHIV value at the end of the previous interval, and inside the interval, SHIV load is described with exponential rate specific for this interval.

For untreated animals, the following model describes SHIV dynamics and is used for data fitting: $dSHIV/dt = ku \times SHIV$ when $0 \leq t < T$, $dSHIV/dt = k \times SHIV$ when $T \leq t$, and $SHIV(0) = SHIV_0$, where ku is the rate of exponential increase of SHIV in plasma before the peak of viremia, k is the rate of exponential decrease of SHIV in plasma after the peak of viremia, T is the time of the peak of viremia, assuming that $T \geq 9$ days, and $SHIV_0$ is the concentration of SHIV in plasma at time zero. In addition, we also analyzed the rate for untreated macaques from day 16 to day 18, as characterized by the rate constant k16u using the same equation but only data for days 16 and 18.

This model consists of two exponential curves, as represented by linear functions in logarithm scale. The first curve describes the exponential increase of SHIV load in plasma with the rate of ku where increase results from infection of new cells and production of SHIV particles by these cells. The second curve describes exponential decrease of SHIV in plasma with the of rate k where decrease results from elimination of infected cells and cell-produced SHIV particles by the immune system and lack of target cells. All four parameters (ku, k, T, and $SHIV_0$) were obtained during the data fitting for untreated macaques.

For treated animals, the model describes 4 treatments at the time points (T) 7, 9, 16, and 18 days: $dSHIV/dt = kt \times SHIV$, $0 \leq t < 7$; $dSHIV/dt = k7 \times SHIV$, $7 \leq t < 9$; $dSHIV/dt = k9 \times SHIV$, $9 \leq t < 16$; $dSHIV/dt = k16 \times SHIV$, $16 \leq t < 18$; and $dSHIV/dt = k18 \times SHIV$, $18 \leq t$; $SHIV(0) = aSHIV_0$. kt is the rate of exponential increase in the interval 0 to 7 days, k7, k9, k16, and k18 are rates of exponential increase/decrease for 7 to 9, 9 to 16, and 16 to 18 days and after 18 days, respectively; and $aSHIV_0$ is the concentration of SHIV plasma load on day 0.

In this model, the initial concentration of SHIV for treated macaques is equal to an average value $aSHIV_0$ calculated for untreated macaques (M): $aSHIV_0 = (SHIV_0$ for M1 + $SHIV_0$ for M2 + $SHIV_0$ for M3 + $SHIV_0$ for M4)/4. This accounts for only one SHIV load value for treated macaques before the treatment (day 7); therefore, it is not possible to determine $SHIV_0$ by data fitting. For untreated macaques, we used two values of SHIV load on days 7 and 9 for extrapolating and defining $SHIV_0$. The rate constant kt describes the increase of SHIV before the first treatment and before the peak, assuming that the peak SHIV load occurs at least on day 9 or later. Therefore, it should have only positive values for all treated macaques. Obviously, we should expect that kt would be approximately the same as ku. The rate constants k7, k9, k16, and k18 describe SHIV dynamics after the corresponding treatments. These constants can have both positive and negative values, depending on the effect of treatment and individual variations in macaques. At different time points, the effects can also be different. Five parameters (kt, k7, k9, 16, and k18) were obtained by the fitting of the data for treated macaques.

ACKNOWLEDGMENTS

We thank members of our groups for help.

This work was supported by the National Natural Science Foundation of China (81822027, 31570936, 81630090, 81501735, 81561128006, and 81601761), the Intramural Research Program of the CCR, the National Cancer Institute, National Institutes of Health (NIH), the Office of AIDS Research at the NIH, and the University of Pittsburgh Medical Center.

REFERENCES

1. Persaud D, Zhou Y, Siliciano JM, Siliciano RF. 2003. Latency in human immunodeficiency virus type 1 infection: no easy answers. J Virol 77:1659–1665. https://doi.org/10.1128/jvi.77.3.1659-1665.2003.
2. Ho YC, Shan L, Hosmane NN, Wang J, Laskey SB, Rosenbloom DIS, Lai J, Blankson JN, Siliciano JD, Siliciano RF. 2013. Replication-competent noninduced proviruses in the latent reservoir increase barrier to HIV-1 cure. Cell 155:540–551. https://doi.org/10.1016/j.cell.2013.09.020.
3. Davey RT, Jr, Bhat N, Yoder C, Chun TW, Metcalf JA, Dewar R, Natarajan V, Lempicki RA, Adelsberger JW, Miller KD, Kovacs JA, Polis MA, Walker RE, Falloon J, Masur H, Gee D, Baseler M, Dimitrov DS, Fauci AS, Lane HC. 1999. HIV-1 and T cell dynamics after interruption of highly active antiretroviral therapy (HAART) in patients with a history of sustained viral suppression. Proc Natl Acad Sci U S A 96:15109–15114. https://doi.org/10.1073/pnas.96.26.15109.
4. Chun TW, Davey RT, Engel D, Lane HC, Fauci AS. 1999. Re-emergence of HIV after stopping therapy. Nature 401:874–875. https://doi.org/10.1038/44755.
5. Dimitrov DS. 2012. Therapeutic proteins. Methods Mol Biol 899:1–26. https://doi.org/10.1007/978-1-61779-921-1_1.
6. Burton DR, Mascola JR. 2015. Antibody responses to envelope glycoproteins in HIV-1 infection. Nat Immunol 16:571–576. https://doi.org/10.1038/ni.3158.
7. Bar KJ, Sneller MC, Harrison LJ, Justement JS, Overton ET, Petrone ME, Salantes DB, Seamon CA, Scheinfeld B, Kwan RW, Learn GH, Proschan MA, Kreider EF, Blazkova J, Bardsley M, Refsland EW, Messer M, Clarridge KE, Tustin NB, Madden PJ, Oden K, O'Dell SJ, Jarocki B, Shiakolas AR, Tressler RL, Doria-Rose NA, Bailer RT, Ledgerwood JE, Capparelli EV, Lynch RM, Graham BS, Moir S, Koup RA, Mascola JR, Hoxie JA, Fauci AS, Tebas P, Chun TW. 2016. Effect of HIV antibody VRC01 on viral rebound after treatment interruption. N Engl J Med 375:2037–2050. https://doi.org/10.1056/NEJMoa1608243.
8. Scheid JF, Horwitz JA, Bar-On Y, Kreider EF, Lu CL, Lorenzi JC, Feldmann A, Braunschweig M, Nogueira L, Oliveira T, Shimeliovich I, Patel R, Burke L, Cohen YZ, Hadrigan S, Settler A, Witmer-Pack M, West AP, Jr, Juelg B, Keler T, Hawthorne T, Zingman B, Gulick RM, Pfeifer N, Learn GH, Seaman MS, Bjorkman PJ, Klein F, Schlesinger SJ, Walker BD, Hahn BH, Nussenzweig MC, Caskey M. 2016. HIV-1 antibody 3BNC117 suppresses viral rebound in humans during treatment interruption. Nature 535:556–560. https://doi.org/10.1038/nature18929.
9. Barouch DH, Whitney JB, Moldt B, Klein F, Oliveira TY, Liu J, Stephenson KE, Chang HW, Shekhar K, Gupta S, Nkolola JP, Seaman MS, Smith KM, Borducchi EN, Cabral C, Smith JY, Blackmore S, Sanisetty S, Perry JR, Beck M, Lewis MG, Rinaldi W, Chakraborty AK, Poignard P, Nussenzweig MC, Burton DR. 2013. Therapeutic efficacy of potent neutralizing HIV-1-specific monoclonal antibodies in SHIV-infected rhesus monkeys. Nature 503:224–228. https://doi.org/10.1038/nature12744.
10. Horwitz JA, Halper-Stromberg A, Mouquet H, Gitlin AD, Tretiakova A, Eisenreich TR, Malbec M, Gravemann S, Billerbeck E, Dorner M, Buning H, Schwartz O, Knops E, Kaiser R, Seaman MS, Wilson JM, Rice CM, Ploss A, Bjorkman PJ, Klein F, Nussenzweig MC. 2013. HIV-1 suppression and durable control by combining single broadly neutralizing antibodies and antiretroviral drugs in humanized mice. Proc Natl Acad Sci U S A 110:16538–16543. https://doi.org/10.1073/pnas.1315295110.
11. Kong R, Louder MK, Wagh K, Bailer RT, deCamp A, Greene K, Gao H, Taft JD, Gazumyan A, Liu C, Nussenzweig MC, Korber B, Montefiori DC, Mascola JR. 2015. Improving neutralization potency and breadth by combining broadly reactive HIV-1 antibodies targeting major neutralization epitopes. J Virol 89:2659–2671. https://doi.org/10.1128/JVI.03136-14.
12. Nishimura Y, Martin MA. 2017. Of mice, macaques, and men: broadly neutralizing antibody immunotherapy for HIV-1. Cell Host Microbe 22:207–216. https://doi.org/10.1016/j.chom.2017.07.010.
13. Asokan M, Rudicell RS, Louder M, McKee K, O'Dell S, Stewart-Jones G, Wang K, Xu L, Chen X, Choe M, Chuang G, Georgiev IS, Joyce MG, Kirys T, Ko S, Pegu A, Shi W, Todd JP, Yang Z, Bailer RT, Rao S, Kwong PD, Nabel GJ, Mascola JR. 2015. Bispecific antibodies targeting different epitopes on the HIV-1 envelope exhibit broad and potent neutralization. J Virol 89:12501–12512. https://doi.org/10.1128/JVI.02097-15.
14. Huang Y, Yu J, Lanzi A, Yao X, Andrews CD, Tsai L, Gajjar MR, Sun M, Seaman MS, Padte NN, Ho DD. 2016. Engineered bispecific antibodies with exquisite HIV-1-neutralizing activity. Cell 165:1621–1631. https://doi.org/10.1016/j.cell.2016.05.024.
15. Chen W, Feng Y, Prabakaran P, Ying T, Wang Y, Sun J, Macedo CD, Zhu Z, He Y, Polonis VR, Dimitrov DS. 2014. Exceptionally potent and broadly cross-reactive, bispecific multivalent HIV-1 inhibitors based on single human CD4 and antibody domains. J Virol 88:1125–1139. https://doi.org/10.1128/JVI.02566-13.
16. Gardner MR, Kattenhorn LM, Kondur HR, von Schaewen M, Dorfman T, Chiang JJ, Haworth KG, Decker JM, Alpert MD, Bailey CC, Neale ES, Jr, Fellinger CH, Joshi VR, Fuchs SP, Martinez-Navio JM, Quinlan BD, Yao AY, Mouquet H, Gorman J, Zhang B, Poignard P, Nussenzweig MC, Burton DR, Kwong PD, Piatak M, Jr, Lifson JD, Gao G, Desrosiers RC, Evans DT, Hahn BH, Ploss A, Cannon PM, Seaman MS, Farzan M. 2015. AAV-expressed eCD4-Ig provides durable protection from multiple SHIV challenges. Nature 519:87–91. https://doi.org/10.1038/nature14264.
17. Davis-Gardner ME, Gardner MR, Alfant B, Farzan M. 2017. eCD4-Ig promotes ADCC activity of sera from HIV-1-infected patients. PLoS Pathog 13:e1006786. https://doi.org/10.1371/journal.ppat.1006786.
18. Bolton DL, Pegu A, Wang KY, McGinnis K, Nason M, Foulds K, Letukas V, Schmidt SD, Chen XJ, Todd JP, Lifson JD, Rao S, Michael NL, Robb ML, Mascola JR, Koup RA. 2016. Human immunodeficiency virus type 1 monoclonal antibodies suppress acute simian-human immunodeficiency virus viremia and limit seeding of cell-associated viral reservoirs. J Virol 90:1321–1332. https://doi.org/10.1128/JVI.02454-15.
19. Nishimura Y, Gautam R, Chun TW, Sadjadpour R, Foulds KE, Shingai M, Klein F, Gazumyan A, Golijanin J, Donaldson M, Donau OK, Plishka RJ, Buckler-White A, Seaman MS, Lifson JD, Koup RA, Fauci AS, Nussenzweig MC, Martin MA. 2017. Early antibody therapy can induce long-lasting immunity to SHIV. Nature 543:559–563. https://doi.org/10.1038/nature21435.
20. Hessell AJ, Jaworski JP, Epson E, Matsuda K, Pandey S, Kahl C, Reed J, Sutton WF, Hammond KB, Cheever TA, Barnette PT, Legasse AW, Planer S, Stanton JJ, Pegu A, Chen X, Wang K, Siess D, Burke D, Park BS, Axthelm MK, Lewis A, Hirsch VM, Graham BS, Mascola JR, Sacha JB, Haigwood NL. 2016. Early short-term treatment with neutralizing human monoclonal antibodies halts SHIV infection in infant macaques. Nat Med 22:362–368. https://doi.org/10.1038/nm.4063.
21. Chen WZ, Zhu ZY, Feng Y, Dimitrov DS. 2008. Human domain antibodies to conserved sterically restricted regions on gp120 as exceptionally potent cross-reactive HIV-1 neutralizers. Proc Natl Acad Sci U S A 105:17121–17126. https://doi.org/10.1073/pnas.0805297105.
22. Meyerson JR, Tran EE, Kuybeda O, Chen W, Dimitrov DS, Gorlani A, Verrips T, Lifson JD, Subramaniam S. 2013. Molecular structures of trimeric HIV-1 Env in complex with small antibody derivatives. Proc Natl Acad Sci U S A 110:513–518. https://doi.org/10.1073/pnas.1214810110.
23. Chen W, Bardhi A, Feng Y, Wang Y, Qi Q, Li W, Zhu Z, Dyba MA, Ying T, Jiang S, Goldstein H, Dimitrov DS. 2016. Improving the CH1-CK heterodimerization and pharmacokinetics of 4Dm2m, a novel potent CD4-antibody fusion protein against HIV-1. MAbs 8:761–774. https://doi.org/10.1080/19420862.2016.1160180.
24. Bardhi A, Wu Y, Chen W, Li W, Zhu Z, Zheng JH, Wong H, Jeng E, Jones J, Ochsenbauer C, Kappes JC, Dimitrov DS, Ying T, Goldstein H. 2017. Potent in vivo NK cell-mediated elimination of HIV-1-infected cells mobilized by a gp120-bispecific and hexavalent broadly neutralizing fusion protein. J Virol 91:e00937-17. https://doi.org/10.1128/JVI.00937-17.
25. Kong D, Wang Y, Ji P, Li W, Ying T, Huang J, Wang C, Wu Y, Wang Y, Chen W, Hao Y, Hong K, Shao Y, Dimitrov DS, Jiang S, Ma L. 2018. A defucosylated bispecific multivalent molecule exhibits broad HIV-1-neutralizing activity and enhanced antibody-dependent cellular cytotoxicity against reactivated HIV-1 latently infected cells. AIDS 32:1749–1761. https://doi.org/10.1097/QAD.0000000000001869.
26. Shingai M, Nishimura Y, Klein F, Mouquet H, Donau OK, Plishka R, Buckler-White A, Seaman M, Piatak M, Jr, Lifson JD, Dimitrov DS, Nussenzweig MC, Martin MA. 2013. Antibody-mediated immunotherapy of macaques chronically infected with SHIV suppresses viraemia. Nature 503:277–280. https://doi.org/10.1038/nature12746.
27. Julg B, Liu PT, Wagh K, Fischer WM, Abbink P, Mercado NB, Whitney JB, Nkolola JP, McMahan K, Tartaglia LJ, Borducchi EN, Khatiwada S, Kamath M, LeSuer JA, Seaman MS, Schmidt SD, Mascola JR, Burton DR, Korber BT, Barouch DH. 2017. Protection against a mixed SHIV challenge by a

broadly neutralizing antibody cocktail. Sci Transl Med 9:eaao4235. https://doi.org/10.1126/scitranslmed.aao4235.
28. Xu L, Pegu A, Rao E, Doria-Rose N, Beninga J, McKee K, Lord DM, Wei RR, Deng G, Louder M, Schmidt SD, Mankoff Z, Wu L, Asokan M, Beil C, Lange C, Leuschner WD, Kruip J, Sendak R, Kwon YD, Zhou T, Chen X, Bailer RT, Wang K, Choe M, Tartaglia LJ, Barouch DH, O'Dell S, Todd JP, Burton DR, Roederer M, Connors M, Koup RA, Kwong PD, Yang ZY, Mascola JR, Nabel GJ. 2017. Trispecific broadly neutralizing HIV antibodies mediate potent SHIV protection in macaques. Science 358:85–90. https://doi.org/10.1126/science.aan8630.
29. Dimitrov DS, Willey RL, Sato H, Chang LJ, Blumenthal R, Martin MA. 1993. Quantitation of human-immunodeficiency-virus type-1 infection kinetics. J Virol 67:2182–2190.
30. Ko S-Y, Pegu A, Rudicell RS, Yang Z-Y, Joyce MG, Chen X, Wang K, Bao S, Kraemer TD, Rath T, Zeng M, Schmidt SD, Todd J-P, Penzak SR, Saunders KO, Nason MC, Haase AT, Rao SS, Blumberg RS, Mascola JR, Nabel GJ. 2014. Enhanced neonatal Fc receptor function improves protection against primate SHIV infection. Nature 514:642–645. https://doi.org/10.1038/nature13612.
31. Rosenberg Y, Sack M, Montefiori D, Labranche C, Lewis M, Urban L, Mao L, Fischer R, Jiang X. 2015. Pharmacokinetics and immunogenicity of broadly neutralizing HIV monoclonal antibodies in macaques. PLoS One 10:e0120451. https://doi.org/10.1371/journal.pone.0120451.
32. Michaud HA, Gomard T, Gros L, Thiolon K, Nasser R, Jacquet C, Hernandez J, Piechaczyk M, Pelegrin M. 2010. A crucial role for infected-cell/antibody immune complexes in the enhancement of endogenous antiviral immunity by short passive immunotherapy. PLoS Pathog 6:e1000948. https://doi.org/10.1371/journal.ppat.1000948.
33. Lambour J, Naranjo-Gomez M, Piechaczyk M, Pelegrin M. 2016. Converting monoclonal antibody-based immunotherapies from passive to active: bringing immune complexes into play. Emerg Microbes Infect 5:e92. https://doi.org/10.1038/emi.2016.97.
34. Kasai N, Yoshikawa Y, Enokizono J. 2014. Effect of antigen-dependent clearance on pharmacokinetics of anti-heparin-binding EGF-like growth factor (HB-EGF) monoclonal antibody. MAbs 6:1220–1228. https://doi.org/10.4161/mabs.29792.
35. Caskey M, Klein F, Lorenzi JC, Seaman MS, West AP, Jr, Buckley N, Kremer G, Nogueira L, Braunschweig M, Scheid JF, Horwitz JA, Shimeliovich I, Ben-Avraham S, Witmer-Pack M, Platten M, Lehmann C, Burke LA, Hawthorne T, Gorelick RJ, Walker BD, Keler T, Gulick RM, Fatkenheuer G, Schlesinger SJ, Nussenzweig MC. 2015. Viraemia suppressed in HIV-1-infected humans by broadly neutralizing antibody 3BNC117. Nature 522:487–491. https://doi.org/10.1038/nature14411.
36. Pegu A, Asokan M, Wu L, Wang K, Hataye J, Casazza JP, Guo X, Shi W, Georgiev I, Zhou T, Chen X, O'Dell S, Todd J-P, Kwong PD, Rao SS, Yang Z-y, Koup RA, Mascola JR, Nabel GJ. 2015. Activation and lysis of human CD4 cells latently infected with HIV-1. Nat Commun 6:8447. https://doi.org/10.1038/ncomms9447.
37. Brozy J, Schlaepfer E, Mueller CKS, Rochat MA, Rampini SK, Myburgh R, Raum T, Kufer P, Baeuerle PA, Muenz M, Speck RF. 2018. Antiviral activity of HIV gp120-targeting bispecific T cell engager antibody constructs. J Virol 92:e00491-18. https://doi.org/10.1128/JVI.00491-18.
38. Jaworski JP, Vendrell A, Chiavenna SM. 2016. Neutralizing monoclonal antibodies to fight HIV-1: on the threshold of success. Front Immunol 7:661. https://doi.org/10.3389/fimmu.2016.00661.
39. Liu L, Patel B, Ghanem MH, Bundoc V, Zheng Z, Morgan RA, Rosenberg SA, Dey B, Berger EA. 2015. Novel CD4-based bispecific chimeric antigen receptor designed for enhanced anti-HIV potency and absence of HIV entry receptor activity. J Virol 89:6685–6694. https://doi.org/10.1128/JVI.00474-15.
40. Bouvin-Pley M, Morgand M, Meyer L, Goujard C, Moreau A, Mouquet H, Nussenzweig M, Pace C, Ho D, Bjorkman PJ, Baty D, Chames P, Pancera M, Kwong PD, Poignard P, Barin F, Braibant M. 2014. Drift of the HIV-1 envelope glycoprotein gp120 toward increased neutralization resistance over the course of the epidemic: a comprehensive study using the most potent and broadly neutralizing monoclonal antibodies. J Virol 88:13910–13917. https://doi.org/10.1128/JVI.02083-14.
41. Fetzer I, Gardner MR, Davis-Gardner ME, Prasad NR, Alfant B, Weber JA, Farzan M. 2018. eCD4-Ig variants that more potently neutralize HIV-1. J Virol 92:e02011-17. https://doi.org/10.1128/JVI.02011-17.
42. Mendoza P, Gruell H, Nogueira L, Pai JA, Butler AL, Millard K, Lehmann C, Suarez I, Oliveira TY, Lorenzi JCC, Cohen YZ, Wyen C, Kummerle T, Karagounis T, Lu CL, Handl L, Unson-O'Brien C, Patel R, Ruping C, Schlotz M, Witmer-Pack M, Shimeliovich I, Kremer G, Thomas E, Seaton KE, Horowitz J, West AP, Jr, Bjorkman PJ, Tomaras GD, Gulick RM, Pfeifer N, Fatkenheuer G, Seaman MS, Klein F, Caskey M, Nussenzweig MC. 2018. Combination therapy with anti-HIV-1 antibodies maintains viral suppression. Nature 561:479–484. https://doi.org/10.1038/s41586-018-0531-2.
43. Polis MA, Sidorov IA, Yoder C, Jankelevich S, Metcalf J, Mueller BU, Dimitrov MA, Pizzo P, Yarchoan R, Dimitrov DS. 2001. Correlation between reduction in plasma HIV-1 RNA concentration 1 week after start of antiretroviral treatment and longer-term efficacy. Lancet 358:1760–1765. https://doi.org/10.1016/s0140-6736(01)06802-7.
44. Dimitrov DS, Martin MA. 1995. HIV results in the frame. CD4+ cell turnover. Nature 375:194–195. (Author reply, 198.) https://doi.org/10.1038/375194b0.
45. Chan KF, Shahreel W, Wan C, Teo G, Hayati N, Tay SJ, Tong WH, Yang Y, Rudd PM, Zhang P, Song Z. 2016. Inactivation of GDP-fucose transporter gene (Slc35c1) in CHO cells by ZFNs, TALENs and CRISPR-Cas9 for production of fucose-free antibodies. Biotechnol J 11:399–414. https://doi.org/10.1002/biot.201500331.
46. Qi Q, Wang Q, Chen W, Du L, Dimitrov DS, Lu L, Jiang S. 2017. HIV-1 gp41-targeting fusion inhibitory peptides enhance the gp120-targeting protein-mediated inactivation of HIV-1 virions. Emerg Microbes Infect 6:e59. https://doi.org/10.1038/emi.2017.46.
47. Davis SJ, Ward HA, Puklavec MJ, Willis AC, Williams AF, Barclay AN. 1990. High level expression in Chinese hamster ovary cells of soluble forms of CD4 T lymphocyte glycoprotein including glycosylation variants. J Biol Chem 265:10410–10418.